

Detection of *Sclerotinia* rot incidence in indian mustard from polar orbiting satellite platform

B. K. Bhattacharya¹, C. Chattopadhyay², S. Dutta¹, R. L. Meena², Sumana Roy², J. S. Parihar¹, N.K. Patel¹

¹Agricultural Resources Group, Space Applications Centre, ISRO, Ahmedabad 380015, India.

²National Research Centre on Rapeseed-Mustard, ICAR, Sewar, Bharatpur 321303, India.

Email: chirantan_cha@hotmail.com

Abstract

Satellite-sensed detection of disease incidence in crops using optical radiometry depends on degree of loss of greenness of canopy based on differentiation of reflectance patterns between disease-free and diseased crop patches. Crop identification and discrimination between crops from polar orbiting Indian satellite sensors with narrow multi-spectral optical bands in green (450-550 nm), red (550-650 nm), near infrared or NIR (650-750 nm), short-wave infrared (1100-1200nm) and middle infrared or MIR (1500-2000 nm) were standardized. This uses digital data from Indian Remote Sensing (IRS) satellite P6 Linear Imaging Self Scanning (LISS)-IV, 1D LISS-III, IRS P6 Advanced Wide Field sensors with spatial resolutions varying 5.6 m-60 m representing field to local scales with repeat visits at 5-25 day intervals. *Sclerotinia* rot (*Sclerotinia sclerotiorum*) is a major soil borne disease in mustard (*Brassica juncea*) causing premature drying of crops that leads to yield losses up to 40% in India. First week of Feb 2005 witnessed cold (max temp: 19-23.1°C; min temp: 1.7-8°C) and humid (morning relative humidity: 97-100%; afternoon relative humidity: 43-79%) spell with sunny (8.0-10.2 hours bright sunshine) days accompanied by night rainfall (2.7 mm) at Bharatpur (27°12'N; 77°27'E), which resulted in high soil moisture and conditions favourable for the disease. Cloud-free hyperion photograph having 7.5 km swath and 142 km long track coverage were acquired on 24 Feb 2005. *Sclerotinia* rot incidence, ranging 10%-60% was recorded from 20 mustard patches along with Global Positioning System coordinates within a study area of 20 km×5 km. Cloud-free LISS-IV (5.6 m) images over Bharatpur were used to identify distribution of mustard patches. Different pigment and water sensitive spectral regions in hyper-spectral bands from hyperion were identified sensitive to *Sclerotinia* incidences by comparing with ground observed incidence with disease-water-stress-index-V [(radiance or R₈₀₀-R₅₅₀)/(R₁₆₆₀+R₆₈₀)] found better correlated with ground truth. This group records the first report of use of data onboard satellite platform for disease detection in India.

Key words: *Brassica juncea*, *Sclerotinia sclerotiorum*, remote sensing, disease detection, hyperspectral band

Introduction

The first spaceborne hyperspectral sensor, Hyperion, was launched by NASA onboard Earth Observing -1 (EO-1). It gathers data in 220 discrete narrow bands along 400-2200 nm spectral range at 30 m spatial resolution in 12 bits radiometry. Each image has 7.5 km swath and 142 km along track coverage. Researchers (Thenkabail et al., 2002) have shown that the narrow wavebands located in specific portions of the spectrum have the ability to provide required information for a given application. There is no single approach to determine the optimal number of narrow bands required to provide the best estimates of agricultural crop statistics (Thenkabail et al., 2002). The potential of high spectral resolution data acquired by EO -1 Hyperion polar orbiting sensor has been demonstrated for disease detection and severity classification of sugarcane orange rust, *Rhizoctonia solani*, (Apan et al., 2004). Spectral reflectance of a crop over spectrally continuous optical bands (300 – 2500nm) can capture the subtle differences between diseased and healthy crops when plotted at band intervals of ≤10 nm. Any substantial change in leaf water content or pigmentation of a stressed crop can be detected due to decrease in reflectance in middle infrared (1200 -2500nm) (MIR) bands and due to shift in red edge in near infrared bands (600 – 750 nm). Vegetation indices (VI) have been used in remote sensing since the early days of Landsat. They are well established tools, simple to implement, can be compared to multispectral data, and for hyperspectral data many VIs can be computed.

Disease forecasts at plot level have been made by many researchers earlier (Jalali, 1999). Application of remote sensing for disease detection has been reported earlier by Kanemasu et al., (1974); Nageswara Rao & Rao (1982); Dutta et al., (2004); Ranganath et al., (2004). The forecast of insect-pest, time of incidence and its spatial locations using remote sensing (RS) data has been demonstrated earlier by Dutta et al., (2004). Validation of the spatial locations is an expensive and time-consuming proposition due to extensive ground truth required for inaccessible area. Complementary to ground truth, the spatial distribution of diseased crop as predicted can be validated using hyperspectral data. Here a simple approach for disease detection on mustard crop has been applied to demonstrate the procedure.

Materials and Methods

The study area is located in Bharatpur district of Rajasthan, India (27.0°-27.25° N, 77.25°-77.5° E). The area selected is predominantly mustard crop growing region representative of semi-arid zones of India. Ground truth observations were taken using GPS locations for various plots in a research farm managed by National Research Centre for Mustard (NRCRM) and farmers' fields with varying levels of disease severity. The disease severity scores were also recorded simultaneously.

Hyperion scene centred over Bharatpur having 7.5 km swath and 142 km along track coverage was acquired on Feb 24, 2005. Multi-date cloud free LISS-IV images were also acquired on Dec 2, 2004, Feb 26, 2005 and Mar 13, 2005.

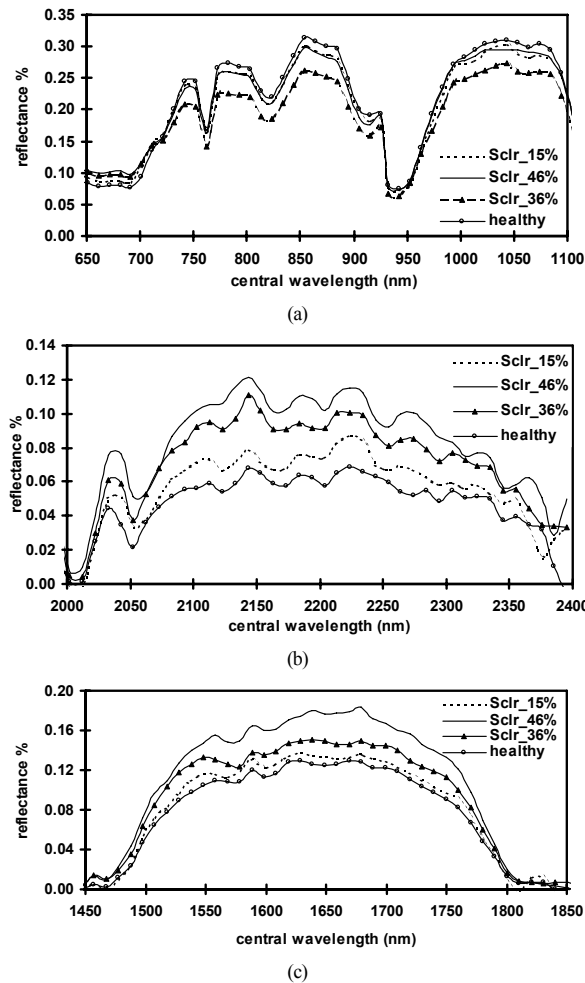


Fig 1: Reflectance spectra for different levels of diseased plots of mustard crop at (a) 650-1100 nm, (b) 1450-1850 nm, (c) 2000-2400 nm

The multi-date IRS LISS-IV data of the study area mentioned above were obtained and geo-registered to sub-pixel accuracy. This was used to delineate mustard crop using hierarchical decision tree based classifier and a mustard crop mask was generated for the study area by excluding all other features. Thereafter, LISS-IV data was re-sampled to 30 m to coincide with the Hyperion data. The Hyperion data was also co-registered with LISS-IV data and was processed to obtain its radiance and converted to top-of-atmosphere-reflectance values. GPS locations of the diseased plots obtained from ground truth were marked in LISS-IV data and then overlaid on the Hyperion data. The spectral response of the diseased crop obtained from hyperspectral data of Hyperion sensor were compared to the disease severities obtained through ground truth. For identification of diseased crops, five Disease-Water-Stress-Indices (DWSI) of Apan et al., (2004) were used, viz., DWSI-1: (R_{800}/R_{1660}) , DWSI-2: (R_{1660}/R_{550}) , DWSI-3: (R_{1660}/R_{680}) , DWSI-4: (R_{550}/R_{680}) , DWSI-5: $[(R_{800}-R_{550})/(R_{1660}+R_{680})]$. Here, the spectral vegetation indices that can distinguish the diseased from healthy crops have been used. In the range from 400-2500 nm the spectra of plants show very distinctive shapes for healthy and diseased crops. Spectral plots showed (Fig. 1a,b,c) that there are other bands than red, that showed inverse relationship with NIR but has greater difference in magnitude i.e., at green (550nm) and at SWIR (1660nm) bands. Thus, it may be better for band rationing to use green-NIR or SWIR-NIR band combinations, rather than the red-NIR bands. The DWSI-1 is the ratio of reflectance in NIR to SWIR, DWSI-2 is the ratio of reflectance in SWIR to Green band, DWSI-3 is the ratio of reflectance in SWIR to Red band, DWSI-4 is the ratio of reflectance in Green to Red band and DWSI-5 is the ratio of reflectance in (NIR-green) to (SWIR + red). The procedure is described (Fig.2).

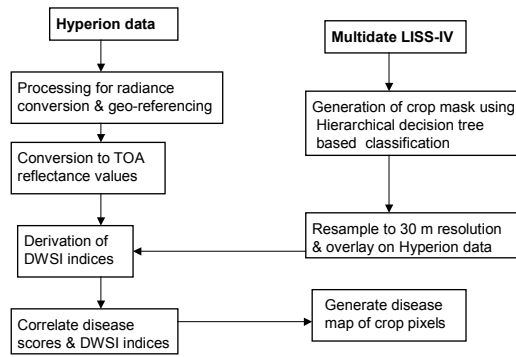


Fig 2: Methodology for disease detection

Resolution analysis of reflectance curves: The significance test for resolution of the spectral curves between healthy and diseased crops was performed in the middle infra-red regions of wavelength i.e., in 1450-1850 nm and 2000-2400 nm ranges (Figs. 1b, c), where the diseased crops can be identified compared to healthy crops. Analysis of the reflectance curves of diseased versus healthy crops was done using student's t-test for paired two sample of means (Anderson, 1972). This was used to determine whether a sample's means were distinct. The combined variance S_c^2 of two samples X_1, X_2 is given by

$$S_c^2 = \frac{S_1^2(n_1 - 1) + S_2^2(n_2 - 1)}{(n_1 - 1) + (n_2 - 1)} \quad (1)$$

where, S_1 and S_2 are the variance and n_1 and n_2 are the sizes of the sample mean μ_1, μ_2 respectively. The standard deviation of the difference of the means S_d is given by

$$S_d = S_c \sqrt{\frac{n_1 + n_2}{n_1 n_2}} \quad (2)$$

$$t = \frac{|\mu_1 - \mu_2|}{S_d} \quad (3)$$

Results and Discussion

Healthy vegetation showed a major increase in reflectance at near infrared and a decrease in middle infrared spectral bands. The chlorophyll absorption occurs broadly in red band at 660-700 nm. The change in absorption is usually large, ranging from a reflectance low of about 7% at 680 nm to a reflectance high of about 30% at 830 nm (Fig. 1a). The absorption in red region at 681 nm decreased with the growth of disease severity. An analysis was done to see how different parts of the reflectance spectrum are affected by disease severity. The green peak at 550 nm is obvious in the plant spectrum as are the chlorophyll absorption (660 nm) and water absorption (970 nm) features. At 1400-1900 nm, water absorption features of the atmosphere are obvious and the reflectance is very low, noisy and is generally removed from graphical presentations for the sake of clarity. Fig. 1b shows the increase in reflectance percentage with increase of disease severity. At 1660 nm, the diseased crops showed sharp increase in reflectance from 0.122 to 0.177% for disease severity level of 0-46%. Similarly, the difference in the spectral profiles of different levels of disease scores can be differentiated very well at 2000-2400 nm (Fig. 1c). The resolution analysis was carried out using equation 1, 2 and 3. At 1660 nm the reflectance of healthy versus diseased crops was seen to be significantly separable (Table 1). The paired t-test analysis showed the means of the spectral curves significantly separable between diseased and healthy crops (Tables 2, 3).

Table 1. Significance test at 1660 nm wavelength between healthy crop and at different levels of disease incidence

| | 15% disease severity | 36% disease severity | 46% disease severity |
|---|----------------------|----------------------|----------------------|
| Standard deviation of two sample means | 0.0013 | 0.0012 | 0.0029 |
| Standard deviation of difference of means | 0.0006 | 0.0006 | 0.0014 |
| Degrees of freedom | 9 | 9 | 9 |
| T calculated | 27.685 | 25.438 | 33.580 |
| T critical at 95% | 0.064 | 0.064 | 0.064 |

The highest difference in reflectance percent was found at 2143 nm channel, among the diseased severity levels of 15, 30 and 46%. The meteorological data obtained during this season showed rainfall occurrence in the previous month. There was

no water scarcity detected during the ground truth visit at this time. The area is irrigated by canal irrigation. Therefore, the stress seen by hyper-spectral data is not due to water scarcity. Among the DWSI indices DWSI-3 (1660/680 nm) was found to best correlated with the disease score with $r^2 = 0.68$ (Fig. 3). The relationship obtained for disease severity with DWSI-3 is: Disease Severity = $1.9688 * \text{DWSI-3} \exp 6.6654$, where $r^2 = 0.68$ $N = 9$. Using this DWSI index and the crop mask generated using LISS-IV data, the diseased pixels within mustard crop were extracted (Fig. 4).

Table 2. Paired t test for two sample of means for diseased vs healthy crops in wavelengths 1450-1850 nm

| | 15% disease severity | 36% disease severity | 46% disease severity | Healthy crop |
|---------------------|----------------------|----------------------|----------------------|--------------|
| Mean | 0.095 | 0.095 | 0.098 | 0.078 |
| Variance | 0.003 | 0.003 | 0.003 | 0.002 |
| Observations | 40 | 40 | 40 | 40 |
| Degrees of freedom | 39 | 39 | 39 | |
| t stat | 13.316 | 13.364 | 12.778 | |
| t critical two-tail | 2.023 | 2.023 | 2.023 | |

Table 3. Paired t test for two sample of means for diseased vs healthy crops in wavelengths 2000-2400 nm

| | 15% disease severity | 36% disease severity | 46% disease severity | Healthy crop |
|---------------------|----------------------|----------------------|----------------------|--------------|
| Mean | 0.072 | 0.071 | 0.082 | 0.047 |
| Variance | 0.001 | 0.001 | 0.001 | 0.001 |
| Observations | 40 | 40 | 40 | 40.000 |
| Degrees of freedom | 39 | 39 | 39 | |
| t stat | 13.104 | 14.843 | 16.478 | |
| t critical two-tail | 2.023 | 2.023 | 2.023 | |

Conclusion

Mustard crop was classified using multi-date IRS LISS_IV data and hierarchical decision tree based classification method. The DWSI indices derived from hyperspectral data were superimposed on the crop mask. The DWSI-3 index (1660/680 nm) showed 68 % correlation with disease score of the mustard crop. The area is irrigated by canal irrigation. Therefore, the stress seen by hyper-spectral data is not due to water scarcity. The DWSI is found to vary in the range 1.4 - 1.7 for disease severity 15-46%. Thus, diseased mustard crop have been discriminated from healthy crop using Hyper-spectral data obtained from Hyperion EO -1 satellite.

Acknowledgement

Authors are grateful to R. R. Navalgund, Director, Space Applications Centre, Ahmedabad for his encouragement and Director, National Research Centre for Rapeseed and Mustard (NRCRM), Bharatpur for supporting this activity.

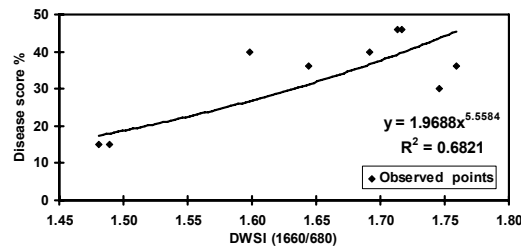


Fig 3. Relationship of DWSI-3 with Sclerotinia rot severities in mustard

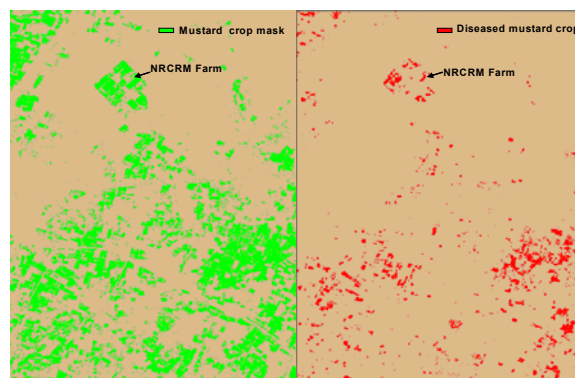


Fig. 4. (a) The mustard crop and (b) the diseased mustard crop at NRCRM, Bharatpur district (27.0°-27.25° N, 77.25°-77.5° E) using Hyperion data

References

- Anderson T.W. (1972). An introduction to multivariate statistical analysis. Wiley Eastern Pub., New Delhi.
- Apan, A., Held, A., Phimm, S., Markley, J. (2004). Detecting sugarcane 'orange rust' disease using EO-1 Hyperion hyperspectral imagery. *Int. J. Remote Sensing*, 25, 489-498.
- Dutta Sujay, Bhattacharya, B. K., Rajak, D.R., Chattopadhyay, C., Vinod Kumar, Roy, S., Sharma, K.C., Dadhwal V. K., Parihar, J.S. (2004). Modelling Regional Level Spatial Distribution of Aphid (*Lipaphis erysimi*) Growth in Indian Mustard Using Satellite Based RS Data. In ISRS Symposium, Jaipur, India, Nov. 3-5, 2004.
- Jalali, B.L. (1999). Computer based decision support system (DSS) and integrated pest management. *J. of Mycology and Pl. Pathology*, 29, 147-158.
- Kanemasu, E.T., Niblett, C.L., Manges, H., Lenhart, D., Newman, M.A. (1974). Wheat: its growth and disease severity as deduced from ERTS-1. *Remote Sensing of Environment*, 3, 255-260.
- Nageswara Rao, P.P., Rao, V.R. (1982). Identification of brown plant hopper and bacterial leaf blight affected rice crop on LANDSAT false colour composites. Proc. 3rd. Asian Conf. Remote Sensing, held at Dhaka, Bangladesh from Dec. 4-7, 1982, pp. 1-12.
- Ranaganth, B.K., Pradeep N., Manjula, V.B., Gowda, B., Ranjana, M.D., Shettigar D., Nageswara Rao, P.P. (2004). Detection of diseased rubber plantations using satellite remote sensing. *J. Indian Soc. of Remote Sensing*, 32, 49-58.
- Thenkabail, P., Smith, R. B., De Pauw, E. (2002). Evaluation of narrow band and broad band vegetation indices for determining optimal hyperspectral wave bands for agricultural crop characterisation. *Photogramm. Engg. & Remote Sensing*, 68, 607-627.